Title	High sensitivity in situ monitoring of NO3 in an atmospheric simulation chamber using incoherent broadband cavity-enhanced absorption spectroscopy
Authors	Venables, Dean S.;Gherman, Titus;Orphal, Johannes;Wenger, John C.;Ruth, Albert A.
Publication date	2006-11
Original Citation	Venables, D. S.,Gherman, T.,Orphal, J.,Wenger, J. C.,Ruth*, A. A.; (2006) 'High sensitivity in situ monitoring of NO3 in an atmospheric simulation chamber using incoherent broadband cavity-enhanced absorption spectroscopy'. Environmental Science & Technology, 40 (21):6758-6763. doi: 10.1021/es061076j
Type of publication	Article (peer-reviewed)
Link to publisher's version	http://pubs.acs.org/doi/abs/10.1021/es061076j - 10.1021/es061076j
Rights	Copyright © 2006 American Chemical Society. This document is the Accepted Manuscript version of a Published Work that appeared in final form in Environmental Science & Technology, copyright © American Chemical Society after peer review and technical editing by the publisher. To access the final edited and published work see http://pubs.acs.org/doi/abs/10.1021/es061076j
Download date	2024-03-29 05:40:10
Item downloaded from	https://hdl.handle.net/10468/795

High sensitivity *in situ* monitoring of NO_3 in an atmospheric simulation chamber using incoherent broadband cavity-enhanced absorption spectroscopy

DEAN S. VENABLES[†], TITUS GHERMAN[‡], JOHANNES ORPHAL[‡,§], JOHN C. WENGER[†], AND ALBERT A. RUTH [*,‡]

Physics Department, National University of Ireland, University College Cork, Ireland,

Chemistry Department, National University of Ireland, University College Cork, Ireland.

Submitted to Environmental Science and Technology, 5 May 2006

[*] Corresponding author: A.A. Ruth, E-mail: a.ruth@ucc.ie, Fax: + 353 21 427 6949.

[†] Chemistry Department. [‡] Physics Department.

[§] Permanent address: Laboratoire Interuniversitaire des Systèmes Atmosphériques, Créteil, France.

We describe the application of Incoherent Broadband Cavity-Enhanced Absorption Spectroscopy (IBBCEAS) for the *in situ* detection of atmospheric trace gases and radicals (NO_3, NO_2, O_3, H_2O) in an atmospheric simulation chamber under realistic atmospheric conditions. The length of the optical cavity across the reaction chamber is 4.5 m, which is significantly longer than in previous studies that use high finesse optical cavities to achieve high absorption sensitivity. Using a straightforward spectrometer configuration, we show that detection limits corresponding to typical atmospheric concentrations can be achieved with a measurement time of seconds to a few minutes. In particular, with only moderate reflectivity mirrors, we report a measured sensitivity of 4 pptv to NO_3 in a 1 minute acquisition time. The high spatial and temporal resolution of the IBBCEAS method and its pptv sensitivity to NO_3 makes it useful in laboratory studies of atmospheric processes as well as having obvious potential for field measurements.

Keywords: Cavity–enhanced, broadband, spectroscopy, atmosphere, trace gases, detection, in situ, ozone, O_3, nitrate, NO_3, NO_2, water, H_2O, arc lamp, IBBCEAS

Introduction

Accurate determination of trace gas and radical concentrations is essential to advance our understanding of chemical processes in the troposphere (1–3). One of the most important tropospheric radicals is the nitrate radical, NO_3 (2). It is the dominant oxidant in the nocturnal troposphere and has been the focus of atmospheric monitoring efforts since the late 1970s (4–6). The early detection of NO_3 in the polluted troposphere (5) and the establishment of its diurnal variation (6) were based on the strong absorption in the electronic B ← X band of NO_3 in the 600–700 nm region (7, 8) and were made using differential optical absorption spectroscopy (DOAS). Long–term DOAS measurements of tropospheric NO_3 started in the mid–1990s (9–13) and focused on several issues including vertical concentration profiles in the urban boundary layer, daytime observations of NO_3 (13), and the role of NO_3 in the marine boundary layer (10). A limitation of DOAS is that it only determines column densities over several kilometers of optical absorption path length; small–scale spatial variations of trace gases cannot be observed with this method. However, recent reviews have emphasized the value of good spatial and temporal resolution in trace gas detection to take account of the variability of the dynamics and chemical composition of the troposphere (14, 15). High spatial and temporal resolution is particularly important for highly reactive species such as NO_3, or those with significant point sources like NO_2. Detection of NO_3 in ambient air with high spatial resolution was first demonstrated in 2000 by King *et al.* using cavity ring–down spectroscopy (CRDS) (16). Several groups have subsequently developed CRD instruments for NO_3 absorption measurements using narrow band lasers (17–19) and broadband light sources (20–22). Recently laser–induced fluorescence (LIF) has also been employed to detect atmospheric NO_3 (23–25), again using the strong electronic transition with maximum at 662 nm. In many cases, the CRDS and LIF instruments can also be used to determine N_2O_5 concentrations, which is in chemical equilibrium with NO_3 and NO_2 under normal conditions (26). Quantifying N_2O_5 provides valuable additional information about tropospheric NO_X chemistry (1–3, 27, 28).

The approach taken in this work uses a broadband light source and a high finesse optical cavity to measure very small absorptions in a gas mixture. Broadband methods have some advantages over narrowband laser methods in the visible and UV owing to their multiplexing capabilities in combination with relatively short data acquisition times. Laser–based broadband methods have recently seen considerable development (29–31). However, a coherent light source is not necessary to take advantage of the increased effective absorption pathlength inside the optical cavity. This was first demonstrated by Fiedler *et al.* (32) who used an incoherent white light source (a Xe arc lamp) in a cavity–enhanced absorption experiment.

In this paper, we describe the first application of incoherent broadband cavity–enhanced absorption spectroscopy (IBBCEAS) to *in situ* measurements of NO_3 in an atmospheric simulation chamber. We demonstrate that IBBCEAS has high sensitivity to typical atmospheric NO_3 concentrations (in the pptv range) together with the advantages of high temporal and spatial resolution. The technique therefore has considerable potential for use in atmospheric simulation chambers, for instance, to allow direct observation of NO_3 in kinetic and mechanistic studies of the oxidation of tropospheric volatile organic compounds (VOC) (33). IBBCEAS also has great potential for deployment in the field, where its high sensitivity to multiple atmospheric species, combined with its high temporal and spatial resolution, will be advantageous in comparison to alternative approaches.

Experiment

The atmospheric simulation chamber used in these experiments has been described in detail elsewhere (34). It consists of a cylindrical teflon vessel with a length of 4.1 m and a diameter of 1.1 m. The chamber has a volume of approximately 3.9 m^3 at atmospheric pressure. It is closed at both ends with teflon foil covered aluminum plates. The chamber is equipped with White–type multiple–reflection optics (35) consisting of three gold–coated mirrors separated by 3.82 m and a total optical path length of 229.6 m (see Figure 1). The White–cell is coupled to a Fourier–transform infrared spectrometer (BioRad Excalibur) to record absorption spectra in the 600–4000 cm^{-1} region with a maximum spectral resolution of 0.25 cm^{-1}. The chamber can be purged with clean air generated by an air purification system (Zander KMA 75) that runs on compressed air and reduces concentrations of NO and NO_2 to less than 1 ppbv. The temperature and humidity in the chamber are monitored with a dewpoint meter (Vaisala DM70). For the measurements described here, a commercial NO_x monitor (Monitor Europe ML 9841B) measured the concentrations of NO_2 and NO.

A scheme of the IBBCEAS setup is shown in Figure 1. Light from a 75 W Xenon short arc lamp (Osram XBO) was focused into a stable optical cavity formed by two high reflectivity dielectric mirrors (Layertec; plane/concave mirrors with a 5 m radius of curvature) at a distance of 462 cm. The mirrors were not purged with an inert gas. The light entering the cavity is spectrally limited by filters to wavelengths greater than 600 nm (Schott RG610 and RG630) and by two irises to reduce stray light. The cavity was aligned using a He–Ne laser and the cavity output was directed into a spectrograph (Oriel MS127i) equipped with a CCD detector (Andor DV401-BV). The spectrograph resolution was better than 0.3 nm, validated using the emission lines of a Sr/Ar hollow cathode lamp. The wavelength scale of the spectrograph and CCD detector was calibrated using an NO_2 spectrum from the literature with a similar spectral resolution to our system (36). The root–mean–square deviation of the calibrated

pixel positions was 0.05 nm. The spectral range covered by the spectrograph and the CCD detector in this study was approximately 130 nm.

In IBBCEAS the reflectivity of the mirrors must be accurately known to obtain quantitative results. We have therefore measured the reflectivity as a function of wavelength using known concentrations of NO_2 and O_3 in the cavity (see Figure 2). Both species absorb across the whole spectral range studied here and their absorption cross–sections are known to high accuracy (36, 37). The NO_2 concentrations were determined using the ML 9841B NO_X monitor, while the O_3 concentrations were obtained from the intergrated area of the FTIR absorption spectrum of the bands around 2100 cm^{-1} using the sum of the O_3 line intensities from the HITRAN database (38) as a reference. Once the number density n [molecules/cm^3] of the species is known, the reflectivity $R(\lambda)$ can be determined by (32):

$$R(\lambda) = 1 - \sigma(\lambda)\, n\, \ell \left(\frac{I_0}{I} - 1 \right)^{-1} \qquad (1)$$

where $\sigma(\lambda)$ is the absorption cross–section of either O_3 or NO_2 from the literature (36, 37, 39), ℓ is the cavity length, and $I(\lambda)$ and $I_0(\lambda)$ are the intensities transmitted by the cavity with and without the absorbing gas present in the cavity. The $R(\lambda)$ values were interpolated using a second–order polynomial; the mirror reflectivity spectrum obtained in this way is shown in Figure 2. The maximum reflectivity obtained at 665 nm is 0.99775 with an estimated uncertainty of 0.00020.

From the reflectivity the effective absorption path length without an absorber present can be estimated from the corresponding ring–down time $\tau_{crd} = \ell\, [c(1\text{-}R)]^{-1}$. Hence the distance travelled within the time τ_{crd} is approximately 2000 m.

Results and Discussion

NO_3 was produced in the atmospheric simulation chamber from the reaction $NO_2 + O_3 \rightarrow NO_3 + O_2$ (26). In order to guarantee a complete NO_2 to NO_3 conversion, we first introduced several ppmv of ozone into the atmospheric simulation chamber. The ozone was produced by an electrical discharge in a constant flow of pure oxygen yielding a mixture of O_3 and O_2. A few ppbv of NO_2 was then added from a small storage bulb that was first filled with a few mbar of NO_2 from a reservoir and then flushed into the simulation chamber with purified air. NO_3 was readily formed due to the large excess of O_3 compared to NO_2. No traces of residual NO_2 were observed in the absorption spectra and N_2O_4 formation was entirely negligible at such low NO_2 concentrations. A typical IBBCEAS spectrum of NO_3 is shown in Figure 3(A). The strongest NO_3 absorption bands (B←X) around 662 and 623 nm dominate the spectrum. The spectrally unresolved absorption bands at 628 and 688 nm shown in Figure 3(A) correspond to the strongly forbidden transitions $b\,^1\Sigma_g^+(v' = 1, 2) \leftarrow X\,^3\Sigma_g^-(v'' = 0)$ (γ– and B– band) of molecular oxygen. The Chappuis absorption band of O_3 also contributes to the observed absorption over the entire spectrum. The ozone absorption spectrum is very smooth in this spectral region and decreases monotonically with increasing wavelength.

To determine experimentally the minimum detectable concentration of NO_3, we purged the atmospheric simulation chamber for about 30 minutes with a flow of purified air. A typical absorption spectrum is shown in Figure 4, illustrating that a concentration of approximately 4 pptv is readily detected in the measurement time of 57 seconds. A nonlinear least squares fit (40) was used to describe the absorption coefficient by:

$$\alpha(\lambda) = n_{O_3}\sigma_{O_3}(\lambda) + n_{NO_3}\sigma_{NO_3}(\lambda) + a \,. \qquad (2)$$

In this equation the number densities n_{O_3} and n_{NO_3} [cm^{-3}] and the constant a [cm^{-1}] are fit parameters, $\sigma_{O_3}(\lambda)$ and $\sigma_{NO_3}(\lambda)$ are taken from the literature for $T = 296$ K (39, 41). The number densities found in the fit were $n_{O_3} = (1.74\pm0.05) \times 10^{12}$ molecules cm^{-3} (≈ 70 ppbv) and $n_{NO_3} = (1.01\pm0.03) \times 10^{8}$ molecules cm^{-3} (≈ 4.1 pptv). The value for a in the fit shown was $(5.24\pm0.12) \times 10^{-9}$ cm^{-1}. The stated uncertainties only represent errors concerning the quality of the fit rather than physical measurement uncertainties. Especially parameter a, which accounts for a constant background due to unavoidable (small) variations in the lamp intensity, can vary from measurement to measurement. In Figure 4 a spectrum by Yokelson et al. (42) is also shown for comparison. This spectrum was scaled down to a mixing ratio of 4.1 pptv to independently confirm the validity of the NO_3 number density obtained in the fit.

The largest contribution to the overall error in the evaluation of concentrations arises from the uncertainty of the term $(1- R(\lambda))$ in Eq. (1) and that of the NO_3 absorption cross–sections $\sigma(\lambda)$. The NO_3 absorption cross–sections are accurate to within 10% (41). The error in $(1- R(\lambda))$ is also approximately 10% using the measured mirror reflectivity $R = 0.99775 \pm 0.00020$. Therefore the estimated maximum uncertainty in the absolute NO_3 concentration is approximately 14%. This uncertainty would always be affected by the same systematic error in $R(\lambda)$ and $\sigma(\lambda)$. The signal–to–noise ratio of the measurement shown in Figure 4 can be estimated from the maximum of the NO_3 absorption $\alpha_{max} = \sigma_{662}\, n_{NO_3} = 2.30\times10^{-9}$ cm^{-1} and the noise in the measurement which is taken as the standard deviation (1σ) of the fit residual ($\sigma \approx 0.33\times10^{-9}$ cm^{-1}, cf. lower panel in Figure 4). With these values the signal–to–noise ratio is approximately $(\alpha_{max}/\sigma) = 7$ in the present measurement. Assuming the detection limit to be three times the noise level of the measurement (3σ), our detection limit for NO_3

is approximately 1.8 pptv corresponding to $\alpha_{min}=1\times10^{-9}$ cm^{-1} for a 1 minute acquisition time. However, we stress that this detection limit is a conservative estimate based on a single spectral point (the absorption maximum at 662 nm); taking account of the full absorption spectrum would give a lower detection limit. Furthermore, with an integration time of 10 minutes for example, the detection limit estimated using the above approach is expected to be about ~0.6 pptv. The determination of relative NO_3 concentrations in long–term time dependent monitoring applications is also better than 1 pptv. The sensitivity of our setup to NO_3 is comparable to reports from the literature but does not require a sophisticated laser system or fast detection electronics (18, 20, 43).

The IBBCEAS detection limit for NO_2 in the same spectral region was estimated (see Figure 3(B) and 5) to be approximately 10 ppbv for an integration time of 57 seconds. This limit implies that typical tropospheric NO_2 concentrations would also be detectable in field measurements using this set of mirrors. The main uncertainty in the measured concentration of NO_2 arises from the uncertainty in the mirror reflectivity, since the NO_2 absorption cross–sections are estimated to be accurate to at least 5% in this spectral range (37). It was not necessary to convolute the NO_2 reference spectrum (36) with our instrument function because the spectral resolution of the reference spectrum is very close to that of our spectrograph/detection system. (The reference spectrum shown in Figure 5 is not an atmospheric spectrum taken from a satellite, but a very accurate reference spectrum of NO_2 taken in the lab).

A practical issue is the presence of H_2O absorption lines in the spectral region of interest, which is well–known in DOAS observations of NO_3. Figure 6 shows the absorption of water in an experiment where the atmospheric simulation chamber was filled overnight with air from the laboratory and the humidity was monitored using the dewpoint meter. The H_2O lines of the HITRAN 2004 database (38) were used to calculate a theoretical spectrum that was convoluted to match the spectral resolution of the spectrograph/detection system. The agreement of both spectra is very good, bearing in mind that no

fitting of the IBBCEAS instrument function has been performed and that other absorbers are also present in the spectrum (see for example the absorption feature at 638 nm). For field experiments, the accurate convolution of the H_2O absorption with the IBBCEAS apparatus function needs to be investigated in greater detail (22). The absorption signature of H_2O may be used to determine the mirror reflectivity and hence the effective absorption path length in a field experiment, even if the strong lines of water are saturated. A convolution of the H_2O with the NO_3 absorption may be less severe at the second strong absorption band of NO_3 at 624 nm. Studies of this kind are in preparation.

Comparison with other methods

The IBBCEAS can be thought of as a hybrid between laser–based cavity–enhanced absorption spectroscopy (CEAS) (where the transmission of an optical cavity is detected) and conventional long–path (differential optical) absorption spectroscopy. Since IBBCEAS has great potential for field deployment as well as for laboratory studies, its advantages and drawbacks in comparison to (A) laser–based CEA techniques and (B) to long–path DOAS methods will be briefly addressed here.

(A) The incoherent broadband approach possesses most of the advantages of cavity–enhanced absorption methods, i.e. high sensitivity, short integration times (seconds to minutes) and compactness of the setup. However, IBBCEAS is experimentally simpler and setups for field experiments are more straightforward to implement in a robust and portable way. The application of a broadband incoherent light source in connection with a spectrograph/CCD detection system has two advantages over laser–based CEAS: (i) Multi-component analysis of spectra is possible due to the multiplexing capability of the method if the concepts of differential optical absorption spectroscopy (DOAS) are applied. (ii) The wavelength region of interest can easily be changed within a wide spectral range from the near UV to near IR.

The most important calibration parameter which needs to be determined accurately for field deployment of IBBCEAS is the mirror reflectivity $R(\lambda) = 1 - T(\lambda) - L(\lambda)$, where T is the mirror transmission and L are the inherent losses of the cavity without the relevant absorbing species present. Even though L is assumed to be generally time independent, small variations of L occur from measurement to measurement due to a gradual accumulation of impurities on the mirrors. This is one of the uncertainties of R as shown in Figure 2 and discussed above. The closer to the time of measurement R can be determined, the smaller will be variations of L and the better is the resulting accuracy of the measurement. In systems employing cavity ring–down spectroscopy, $R(\lambda)$ can in principle be determined from the ring–down time in clean air. In CRD applications not using an open path NO_3 is removed by reaction with NO to establish an absorption baseline. In IBBCEAS, $R(\lambda)$ can be obtained from a known concentration of a molecular species that absorbs in the same spectral range as the target compound. For monitoring NO_3 possible species for the reflectivity calibration are H_2O, O_2, NO_2, or O_3 (as demonstrated in this paper). For example, water concentrations could be determined by a calibrated hygrometer. A drawback of the IBBCEAS approach is the generally lower spectral resolution compared to laser–based methods. A high spectral resolution increases the selectivity of the approach and facilitates the spectral analysis, provided the absorbing gases exhibit highly structured spectra like for instance most atmospheric species in the IR.

(B) IBBCEAS can also be compared to long–path DOAS, which has been used in the field for several decades. The principles of the spectral evaluation procedure are very similar (40). Single– or two–pass DOAS setups are limited to large sample volumes and therefore provide only information on the column densities of trace species. Absorption measurements requiring high spatial resolution, for instance those affected by spatially confined photochemistry or on highly localized radical sources or sinks, are not possible with the long–path DOAS approach. In this context IBBCEAS can be best compared to DOAS

setups coupled to multi–reflection cells, which possess a better spatial resolution and have been employed in conjunction with atmospheric simulation chambers (44, 45). Using an optically stable resonator in IBBCEAS rather than a White– or Herriott–type multi–pass setup offers the advantage of simpler alignment procedures while retaining good spatial resolution and a sensitivity comparable to long–path DOAS. Furthermore, an apparatus based on IBBCEAS has a better portability than a long–path (single– or two–pass) DOAS system and only a single site is required. IBBCEAS can also be used in certain atmospheric applications where the air is sampled and pretreated to remove aerosols, allowing continued observations during periods of precipitation or low visibility. In the specific case of NO_3 monitoring, it would be possible to thermally decompose N_2O_5 to detect this species, as some CRDS and LIF systems have demonstrated (18, 28).

Conclusions

Because many important species involved in tropospheric chemistry have abundances in the ppbv to sub–pptv range, quantifying the mixing ratios of relevant species such as NO_3 requires extremely high sensitivity techniques. Incoherent broadband cavity–enhanced absorption spectroscopy (IBBCEAS) is a highly sensitive method for *in situ* monitoring of NO_3 between 620 and 690 nm. We have demonstrated that concentrations in the pptv range can be measured with an absolute accuracy of approximately 14% (dominated by systematic uncertainties from the mirror reflectivity and the absorption cross–sections of NO_3) and with a relative precision of better than 1 pptv, in an integration time of about one minute. In the same spectral region, NO_2 can also be detected with a sensitivity of tens of ppbv and the absorption of H_2O and O_3 can be utilized for the spectral analysis. This method therefore has considerable potential for field measurements and for kinetic and mechanistic studies of NO_3 reactions at typical atmospheric concentrations. By employing dielectric mirrors with high reflectivity in different spectral regions, the

same instrument can in principle also be used to monitor halogen oxides or other tropospheric species such as HONO or H_2CO. The potential of IBBCEAS for field deployment and its advantages for measuring small scale spatial variations in the composition of the troposphere are also apparent.

Acknowledgments

Support from the European Marie Curie ToK scheme under Framework 6 (grant no: MTKD–CT–2004–014406, "Transfer of Expertise in Atmospheric Monitoring of Urban Pollutants") and from the Irish Research Council for Science Engineering and Technology (SC/2002/160) is gratefully acknowledged.

Literature Cited

1. Monks, P. S. Gas phase radical chemistry in the troposphere. *Chem. Soc. Rev.* **2005**, *34*, 376–395.

2. Wayne, R. P.; Barnes, I.; Biggs, P.; Burrows, J. P.; Canosa-Mas, C. E.; Le Bras, G.; Moortgat, G. K.; Perner, D.; Poulet, G.; Restelli, G.; Sidebottom, H. The nitrate radical – physics, chemistry, and the atmosphere. *Atm. Environ. A* **1991**, *25*, 1–203.

3. Clemitshaw, K. C. A review of instrumentation and measurement techniques for ground-based and airborne field studies of gas-phase tropospheric chemistry. *Critic. Rev. Environ. Sci. Technol.* **2004**, 34, 1–108.

4. Noxon, J. F.; Norton, R. B.; Henderson, W. R. Observation of atmospheric NO_3. *Geophys. Res. Lett.* **1978**, *5*, 675–678.

5. Platt, U.; Perner, D.; Winer, A. M.; Harris, G. W.; Pitts, J. N. Detection of NO_3 in the polluted troposphere by differential optical absorption. *Geophys. Res. Lett.* **1980**, *7*, 89–92.

6. Platt, U.; Perner, D.; Schroder, J.; Kessler, C.; Toenissen, A. The diurnal variation of NO_3. *J. Geophys. Res.* **1981**, *86*, 1965–1970.

7. Jones, E. J.; Wulf, O. R. The absorption coefficient of nitrogen pentoxide in the ultraviolet and the visible spectrum of NO_3. *J. Chem. Phys.* **1937**, *5*, 873–877.

8. Graham, R. A.; Johnston, H. S. The photochemistry of NO_3 and the kinetics of the N_2O_5–O_3 system. *J. Phys. Chem.* **1978**, *82*, 254–268.

9. Heintz, F.; Platt, U.; Flentje, H.; Dubois, R. Long–term observation of nitrate radicals at the Tor station, Kap Arkona (Rügen). *J. Geophys. Res. D* **1996**, *101*, 22891–22910.

10. Allan, B. J.; Carslaw, N.; Coe, H.; Burgess, R. A.; Plane, J. M. C. Observations of the nitrate radical in the marine boundary layer. *J. Atm. Chem.* **1999**, *33*, 129–154.

11. Fish, D. J.; Shallcross, D. E.; Jones, R. L. The vertical distribution of NO_3 in the atmospheric boundary layer. *Atm. Environ.* **1999**, *33*, 687–691.

12. Allan, B. J.; Plane, J. M. C.; Coe, H.; Shillito, J. Observations of NO_3 concentration profiles in the troposphere. *J. Geophys. Res. D* **2003**, *107*, Art. No. 4588.

13. Geyer, A.; Alicke, B.; Ackermann, R.; Martinez, M.; Harder, H.; Brune, W.; Di Carlo, P.; Williams, E.; Jobson, T.; Shetter, R.; Stutz, J. Direct observations of daytime NO_3: Implications for urban boundary layer chemistry. *J. Geophys. Res. D* **2003**, *108*, Art. No. 4368.

14. Ravishankara, A.R. Chemistry-climate coupling: the importance of chemistry in climate issue. *Faraday Disc.* **2005**, *130*, 9–26.

15. Platt, U. Modern methods of the measurement of atmospheric trace gases. *Phys. Chem. Chem. Phys.* **1999**, *1*, 5409–5415.

16. King, M. D.; Dick, E. M.; Simpson, W. R. A new method for atmospheric detection of the nitrate radical (NO_3). *Atm. Environ.* **2000**, *34*, 685–688.

17. Ayers, J. D.; Apodaca, R. L.; Simpson, W. R.; Baer, D. S. Off–axis cavity ringdown spectroscopy: application to atmospheric nitrate radical detection. *Appl. Opt.* **2005**, *44*, 7239–7242.

18. Brown, S. S.; Stark, H.; Ciciora, S. J.; McLaughlin, R. J.; Ravishankara, A. R. Simultaneous in situ detection of atmospheric NO_3 and N_2O_5 via cavity ring–down spectroscopy. *Rev. Sci. Instrum.* **2002**, *73*, 3291–3301.

19. Brown, S. S.; Osthoff, H. D.; Stark, H.; Dube, W. P.; Ryerson, T. B.; Warneke, C.; De Gouw, J. A.; Wollny, A. G.; Parrish, D. D.; Fehsenfeld, F. C.; Ravishankara, A. R. Aircraft observations of daytime NO_3 and N_2O_5 and their implications for tropospheric chemistry. *J. Photochem. Photobiol. A* **2005**, *176*, 270–278.

20. Ball, S. M.; Povey, I. M.; Norton, E. G.; Jones, R. L. Broadband cavity ringdown spectroscopy of the NO_3 radical. *Chem. Phys. Lett.* **2001**, *342*, 113–120.

21. Ball, S.M.; Langridge, J.M.; Jones, R.M.; Broadband cavity enhanced absorption spectroscopy using light emitting diodes. *Chem. Phys. Lett.* **2004**, *398*, 68-74.

22. Bitter, M.; Ball, S. M.; Povey, I. M.; Jones, R. L. A broadband cavity ringdown spectrometer for in situ measurements of atmospheric trace gases. *Atmos. Chem. Phys. Discuss.* **2005**, *5*, 3491–3532.

23. Wood, E. C.; Woolridge, P. J.; Freese, J. H.; Albrecht, T.; Cohen, R. C. Prototype for in situ detection of atmospheric NO_3 and N_2O_5 via laser–induced fluorescence. *Env. Sci. Technol.* **2003**, *37*, 5732–5738.

24. Matsumuto, J.; Kosugi, N.; Imai, H.; Kajii, Y. Development of a measurement system for nitrate radical and dinitrogen pentoxide using a thermal conversion/laser–induced fluorescence technique. *Rev. Sci. Instrum.* **2005**, *76*, 064101.

25. Kim, B.; Hunter, P. L.; Johnston, H. S. NO_3 radical studied by laser–induced fluorescence. *J. Chem. Phys.* **1992**, *96*, 4057–4067.

26. Atkinson, R.; Baulch, D. L.; Cox, R. A.; Crowley, J. N.; Hampson, R. F.; Hynes, R. G.; Jenkin, M. E.; Rossi, M. J.; Troe, J. Evaluated kinetic and photochemical data for atmospheric chemistry: Volume I – gas phase reactions of O_x, HO_x, NO_x and SO_x species. *Atm. Chem. Phys.* **2004**, *4*, 1461–1738.

27. Brown, S. S.; Stark, H.; Ryerson, T. B.; Williams, E. J.; Nicks, D. K.; Trainer, M.; Fehsenfeld, F. C.; Ravishankara, A. R. Nitrogen oxides in the nocturnal boundary layer: Simultaneous in situ measurements of NO_3, N_2O_5, NO_2, NO, and O_3. *J. Geophys. Res. D* **2003**, *108*, Art. No. 4299.

28. Brown, S. S.; Stark, H.; Ravishankara, A. R. Applicability of the steady state approximation to the interpretation of atmospheric observations of NO_3 and N_2O_5. *J. Geophys. Res. D* **2003**, *108*, Art. No. 4539.

29. Ball, S. M.; Jones, R. L. Broadband cavity ring–down spectroscopy. *Chem. Rev.* **2003**, *103*, 5239–5262.

30. Gherman, T; Romanini, D. Mode–locked cavity–enhanced absorption spectroscopy. *Optics Express* **2002**, *10*, 1033–1042.

31. Thorpe, M. J.; Moll, K. D.; Jones, R. J.; Safdi, B.; Ye, J. Broadband cavity ringdown spectroscopy for sensitive and rapid molecular detection. *Science* **2006**, *311*, 1595–1599.

32. Fiedler, S. E.; Hese, A.; Ruth, A. A. Incoherent broadband cavity–enhanced absorption spectroscopy. *Chem. Phys. Lett.* **2003**, *371*, 284–294.

33. Clifford, G. M.; Thüner, L. P.; Wenger, J. C.; Shallcross, D. E. Kinetics of the gas–phase reactions of OH and NO_3 radicals with aromatic aldehydes. *J. Photochem. Photobiol. A* **2005**, *176*, 172–182.

34. Thüner, L. P.; Bardini, P.; Rea, G. J.; Wenger, J. C. Kinetics of the gas–phase reactions of OH and NO_3 radicals with dimethylphenols. *J. Phys. Chem. A* **2004**, *108*, 11019–11025.

35. White, J. U. Long optical paths of large aperture. *J. Opt. Soc. Am.* **1942**, *32*, 285–288.

36. Burrows, J. P.; Dehn, A.; Deters, B.; Himmelmann, S.; Richter, A.; Voigt, S.; Orphal, J. Atmospheric remote–sensing reference data from GOME: 1. Temperature–dependent absorption cross–sections of NO_2 in the 231–794 nm range. *J. Quant. Spectrosc. Rad. Trans.* **1998**, *60*, 1025–1031.

37. Orphal, J. A critical review of the absorption cross–sections of O_3 and NO_2 in the 240–790 nm region. *J. Photochem. Photobiol. A* **2003**, *157*, 185–209.

38. Rothman, L. S.; Jacquemart, D.; Barbe, A.; Benner, D. C.; Birk, M.; Brown, L. R.; Carleer, M. R.; Chackerian Jr., C.; Chance, K. V.; Dana, V.; Devi, V. M.; Flaud, J.–M.; Gamache, R. R.; Goldman, A.; Hartmann, J.–M.; Jucks, K. W.; Maki, A. G.; Mandin, J.–Y.; Massie, S.; Orphal, J.; Perrin, A.; Rinsland, C. P.; Smith, M. A. H.; Toth, R. A.; Vander Auwera, J.; Varanasi, P.; Wagner, G. The HITRAN 2004 molecular spectroscopic database. *J. Quant. Spectrosc. Rad. Trans.* **2005**, *96*, 139–204.

39. Burrows, J. P.; Richter, A.; Dehn, A.; Deters, B.; Himmelmann, S.; Voigt, S.; Orphal, J. Atmospheric remote–sensing reference data from GOME: 2. Temperature–dependent absorption cross–sections of O_3 in the 231–794 nm range. *J. Quant. Spectrosc. Rad. Trans.* **1999**, *61*, 509–517.

40. Stutz, J; Platt, U.; Numerical analysis and estimation of the statistical error of differential optical absorption spectroscopy measurements with least-squares methods. *Appl. Opt.* **1996**, *35*, 6041-6053.

41. Orphal, J.; Fellows, C. E.; Flaud, P. M. The visible absorption spectrum of NO_3 measured by high–resolution Fourier transform spectroscopy. *J. Geophys. Res. D* **2003**, *108*, 4077–4087.

42. Yokelson, R. J.; Burkholder, J. B.; Fox, R. W.; Talukdar, R. K.; Ravishankara, A. R. Temperature dependence of the NO_3 absorption spectrum. *J. Phys. Chem.* **1994**, *98*, 13144–13150.

43. Simpson, W. R. Continuous wave cavity ring–down spectroscopy applied to in situ detection of dinitrogen pentoxide (N_2O_5). *Rev. Sci. Instrum.* **2003**, *74*, 3442–3452.

44. Kurtenbach, R.; Ackermann, R.; Becker, K.H.; Geyer, A.; Gomes, J.A.G.; Lörzer, J.C.; Platt, U.; Wiesen, P. Verification of the contribution of vehicular traffic to the total NMVOC emissions in Germany and the importance of the NO_3 chemistry in the city air. *J. Atmos. Chem.* **2002**, *42*, 395–411.

45. Volkamer, R.; Klotz, B.; Barnes, I.; Imamura, T.; Wirtz, K.; Washida, N.; Becker, K.H.; Platt, U. OH-initiated oxidation of benzene Part I. Phenol formation under atmospheric conditions. *Phys. Chem. Chem. Phys.* **2002**, *4*, 1598–1610.

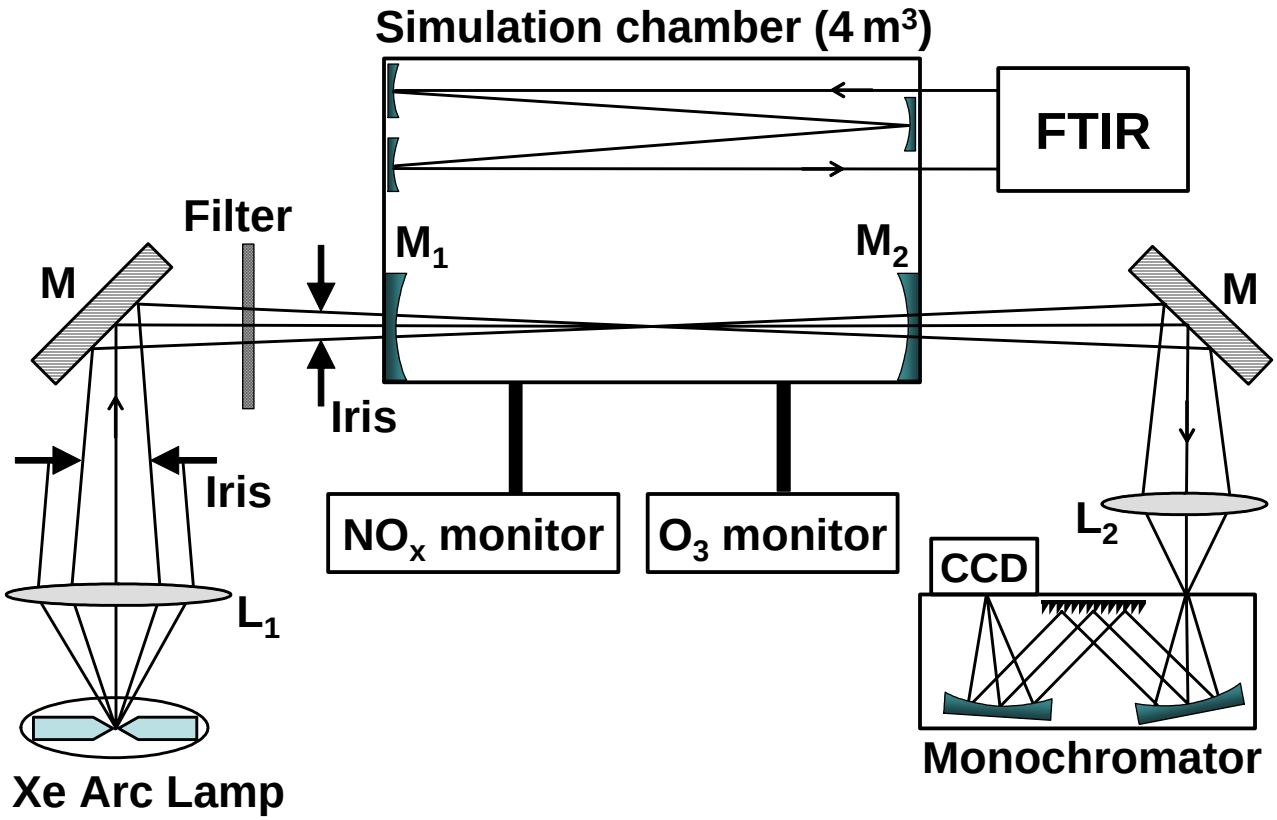

FIGURE 1. Schematic diagram of the experimental setup. L_1 and L_2: lenses; M: metallic mirrors; M_1 and M_2: high reflectivity dielectric mirrors with $R \approx 0.99775$ at 665 nm; Filters: Schott RG 610 and RG 630 of 1mm and 3 mm, respectively; FTIR: Fourier Transform Infrared spectrometer.

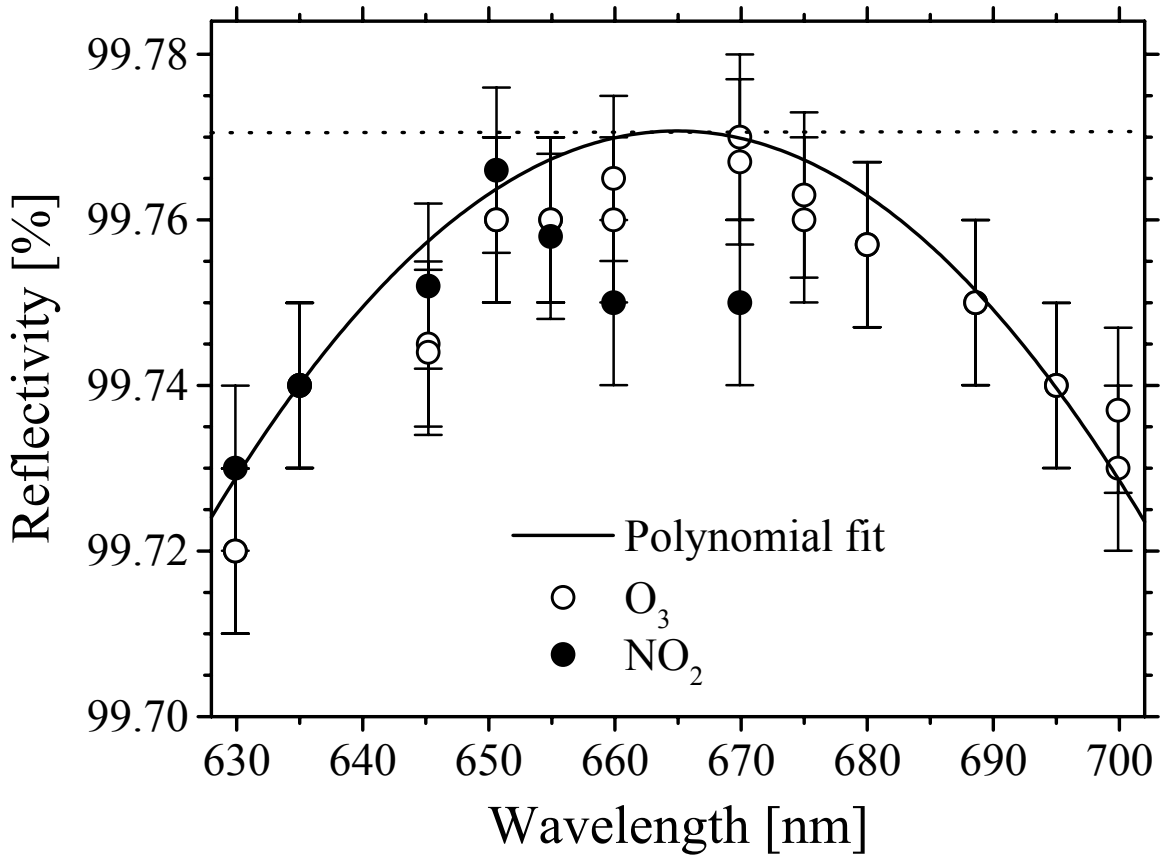

FIGURE 2. The experimentally determined reflectivity as a function of wavelength in the 625–705 nm range. The solid line represents a second–order polynomial fit to the reflectivity values which were determined using concentrations of O_3 (open circles) and NO_2 (solid circles). The O_3 and NO_2 concentrations were determined with the FTIR spectrometer and NO_X monitor respectively (see Figure 1). The dotted horizontal line corresponds to a maximum reflectivity of R=0.99775 at 665 nm. The error bars indicate an estimated uncertainty of ±0.00020.

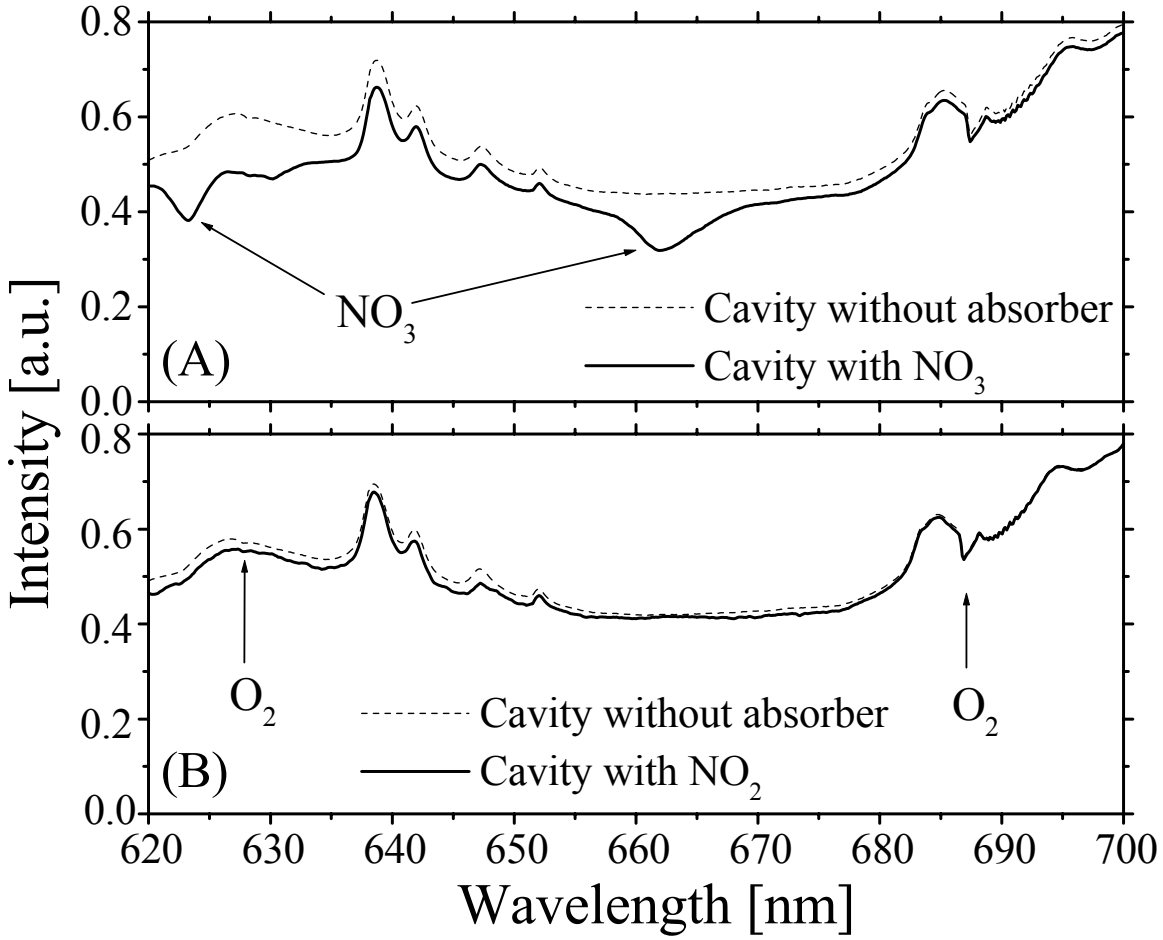

FIGURE 3. Intensity transmitted by the optical cavity: integration time 57 seconds (corresponding to an average of 3000 single readouts of the CCD array with an individual exposure time of 19 ms). (A) The upper panel shows the effect of NO_3 absorption. The simulation chamber was filled with O_3 (ca. 9 ppmv) in large excess of NO_2 prior to the measurement. (B) Shows the effect of filling the cavity with 0.17 ppmv of NO_2. Weak oxygen bands around 688 nm (b(1,0)←X) and 628 nm (b(2,0)←X band) are indicated by vertical arrows. The structure between 635 and 655 nm in (A) and (B) is due to insufficiently suppressed UV emission from the Xe lamp leaking into the detector via the second order of the spectrograph.

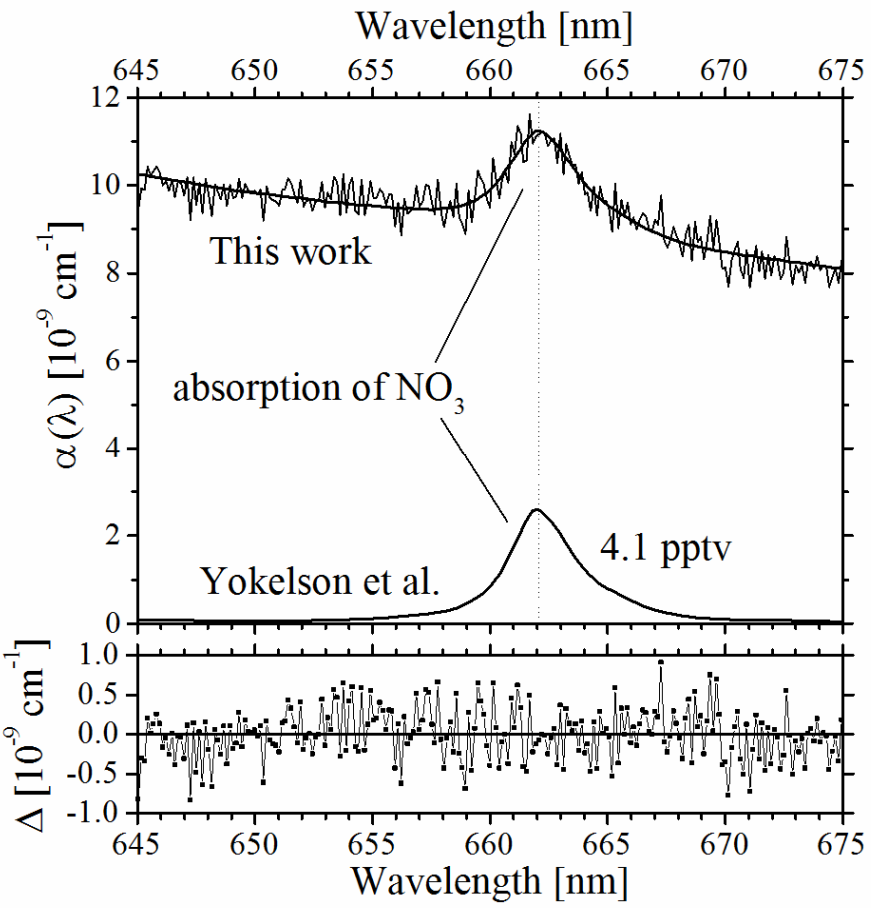

FIGURE 4. Detection of trace amounts of NO_3 in the atmospheric simulation chamber. Upper panel: The data in the upper curve (denoted "this work") were recorded with an integration time of 57 seconds. The minimum detectable concentration of NO_3 with this integration time is estimated to be better than 1 pptv. The upper solid line was calculated using equation (2) with the parameters given in the text. The offset is due to ozone absorption in the atmospheric simulation chamber. The lower curve shows a spectrum of NO_3 by Yokelson et al. (39) scaled to a mixing ratio of 4.1 pptv to match our NO_3 spectrum. Lower panel: Absolute deviation, Δ, between the measured and calculated values of the absorption coefficient.

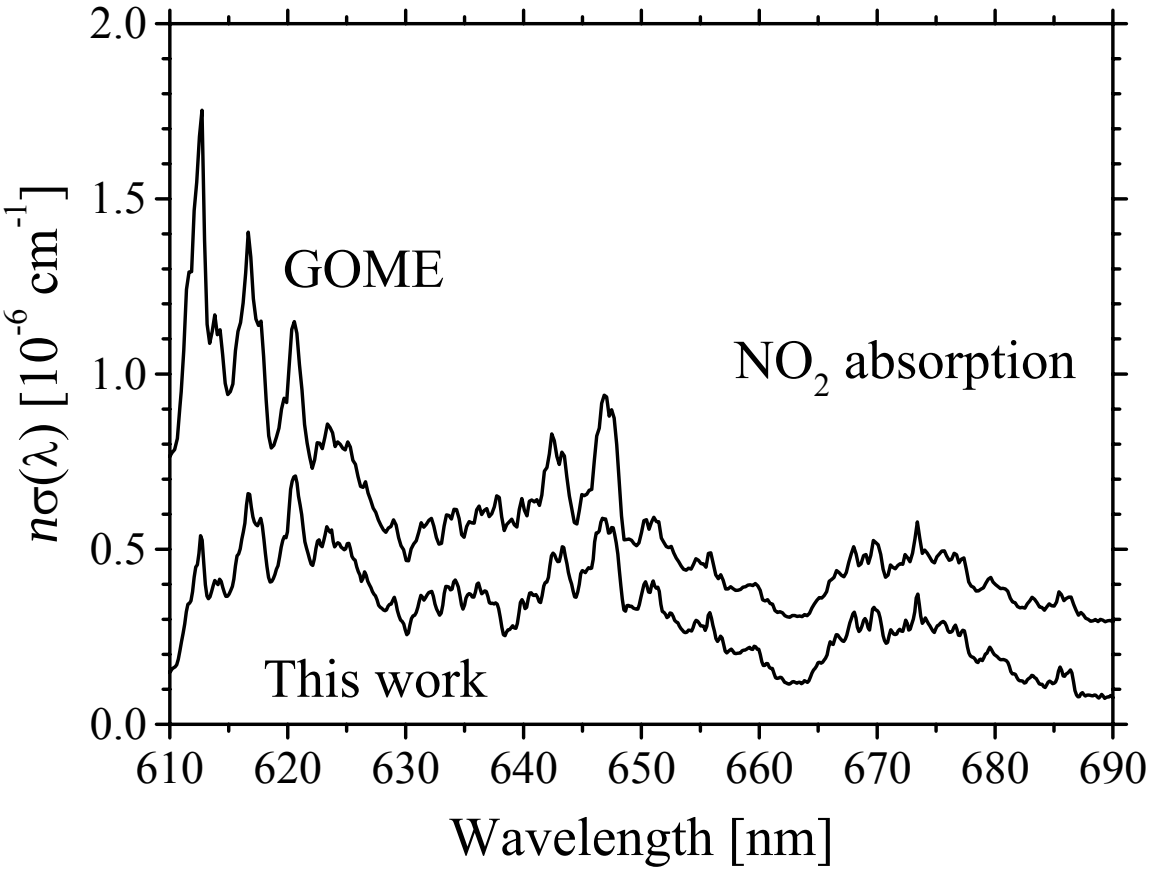

FIGURE 5. Comparison of NO_2 absorption spectra (a) recorded with the IBBCEAS system in an atmospheric simulation chamber (lower trace), and (b) taken with the GOME spectrometer (34) (upper trace). The GOME NO_2 reference spectrum, taken with the GOME-FM in the lab before launch of the mission, was shifted upwards for clarity. Note that the IBBCEAS data fall off in the region of lower mirror reflectivity, i.e. below 620 nm and above 708 nm. Our spectrum was obtained assuming a constant reflectivity over the entire range, leading to slightly distorted features around 645 nm. The detection limit for NO_2 is estimated to be better than 10 ppbv for an integration time of 57 seconds. The

NO_2 absorption features were used for the wavelength calibration of the spectra with an accuracy of about 0.05 nm (RMS).

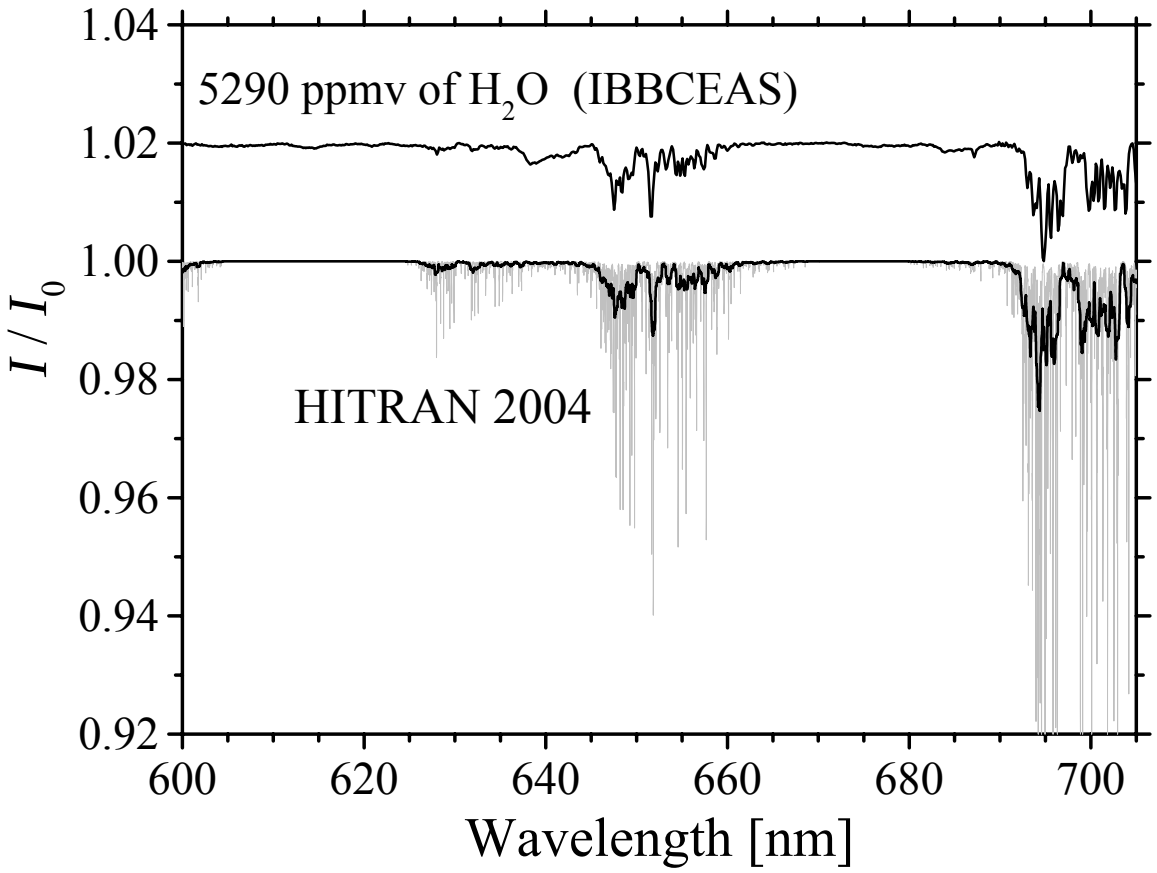

FIGURE 6. Comparison of H_2O absorption spectra recorded with IBBCEAS in an atmospheric simulation chamber (upper trace), and calculated using the HITRAN 2004 database (36) (lower trace). The grey line shows the high–resolution HITRAN spectrum, the black line shows the reference spectrum reduced to instrumental resolution. The IBBCEAS spectrum was shifted upwards by 0.02 for clarity. Note the presence of other absorbers (for example O_2 at 688 nm) in the IBBCEAS spectrum. The HITRAN spectrum was calculated for an effective optical pathlength of 3000 m.